MALDI-TOF-MS unveils the distribution of oligosaccharides produced by hydrolysis of lichen polysaccharides through acidic and oxidative methods – a comparative study

Camille Guitteny, Simon Ollivier, Oznur Yeni, Mathis Ralaivao, Mathieu Fanuel, Joël Boustie, Isabelle Compagnon, Vincent Ferrières, Solenn Ferron, Hélène Rogniaux, et al.

International Journal of Mass Spectrometry 515 (2025) 117473

Contents lists available at ScienceDirect

International Journal of Mass Spectrometry

journal homepage: www.elsevier.com/locate/ijms

MALDI-TOF-MS unveils the distribution of oligosaccharides produced by hydrolysis of lichen polysaccharides through acidic and oxidative methods – a comparative study

Camille Guitteny [a,b], Simon Ollivier [c,d], Oznur Yeni [e], Mathis Ralaivao [a,b], Mathieu Fanuel [c,d], Joël Boustie [b], Isabelle Compagnon [e], Vincent Ferrières [a], Solenn Ferron [b], Hélène Rogniaux [c,d], David Ropartz [c,d], Laurent Legentil [a,*,1], Françoise Le Dévéhat [b,**,1]

[a] Univ Rennes, Ecole Nationale Supérieure de Chimie de Rennes, CNRS, ISCR – UMR6226, F-35000, Rennes, France
[b] Univ Rennes, CNRS, ISCR – UMR 6226, F-35000, Rennes, France
[c] INRAE, UR BIA, F-44316, Nantes, France
[d] INRAE, PROBE Research Infrastructure, BIBS Facility, F-44316, Nantes, France
[e] Univ Lyon, Université Claude Bernard Lyon 1, CNRS, Institut Lumière Matière, Villeurbanne, F69622, France

ARTICLE INFO

Keywords:
Lichen
Polysaccharide
Hydrolysis
MALDI-TOF MS

ABSTRACT

MALDI-TOF MS methods coupled with offline chromatographic data were used to compare the distribution of oligosaccharides generated from acidic or oxidative degradation (Fitdog) of high molecular weight polysaccharides (>10 kDa) obtained from two lichens *Lasallia pustulata* and *Cetraria islandica*. MALDI allowed to quickly compare the kinetics of degradation on both models (starting from non-purified polysaccharides) and to evaluate the dispersity of the resulting oligosaccharides. MALDI-MS confirmed on one hand that TFA hydrolysis gave neutral oligosaccharides easy to correlate with the chemical formula. On the other hand, more structural diversity was evidenced using the Fitdog protocol. Deep analysis of the MALDI data highlighted the formation of by-products corresponding to modified oligosaccharides (e.g., intracyclic cleavages).

1. Introduction

Polysaccharides are ubiquitous carbohydrates found in all kingdoms whether from mammals, algae, fungi, plants or bacteria … They are crucial building blocks of cell walls but they constitute also energy storage [1]. Their industrial use grew up about 17 % between 2017 and 2021 and the major sources of polysaccharides comes from plants (starch, cellulose, inulin or pectin), from marine organisms (chitin/-chitosan or hyaluronic acid) [1] but also from algal sources [2]. In addition to their use to produce energy, they are used in the food, cosmetic and pharmaceutical industries for their properties as absorbents, emulsifiers, stabilizers but also for their biological and active properties [1]. They are deemed to as immunomodulator, antitumor, antiviral as well as antioxidant [2]. More recently, developed research is focused on new vectors for drug delivery made with polysaccharides. They are indeed biocompatible and biodegradable components and they can be used in nanoformulations [3] but they are also used as carriers for osteogenic components in biomedical applications [1]. Yet discovering new polysaccharides is also crucial because some of them are involved in pathogenic virulence and correlating these various biological activities to their chemical structures can be a way to fight against infections [4]. In this context, the underexplored organisms lichens are not left out and deserve to be studied.

Lichens are a stable mutualistic symbiosis between a photobiont, which is an eukaryotic algae (phycobiont) or a cyanobacteria (cyanobiont), and a mycobiont (fungus) which surrounds thanks to its hyphae, the photobiont. The photosynthetic partner produces carbohydrates which are used by the mycobiont for its metabolism. This symbiotic relationship is essential for the tolerance to extreme environments where competition for essential resources like water, light and space is high. Indeed, lichens are poïkilohydric organisms that can survive in habitats with low water retention like rock surfaces, sand, tree trunk, …

* Corresponding author.
** Corresponding author.
E-mail address: francoise.le-devehat@univ-rennes.fr (F. Le Dévéhat).
[1] the authors contributed equally to this work.

https://doi.org/10.1016/j.ijms.2025.117473
Received 4 December 2024; Received in revised form 26 April 2025; Accepted 27 May 2025
Available online 6 June 2025

In the literature, about 60 articles deal with chemical studies on lichen polysaccharides and in most cases, the goal of the authors was to use polysaccharides as taxonomic markers [5] to complement the parallel classification based on polyphenolic compounds. The characterization of the polysaccharides was exclusively realized after an acid hydrolysis in sulfuric acid or trifluoroacetic acid (TFA) or after alkaline hydrolysis followed by gas chromatography-mass spectrometry (GC-MS) after permethylation. The major polysaccharides reported for lichens are linear α-D-glycopyranans (α−(1 → 3)- and (α−(1 → 4)-glucans like isolichenan or nigeran) [5] but also linear β-D-glycopyranans like pustulan described for example in *Lasallia pustulata* [6]. Some heteropolysaccharides (glycans that contain at least two different monosaccharide units) were as well reported in about 20 lichen species and galactomannans with a backbone of α−(1 → 6)-mannose partially substituted at position 2 and 4 by galactofuranose and/or mannopyranose side chains of variable length was studied in *L. pustulata* [5–7,9]. In the same manner, *Cetraria islandica* was described as containing lichenan, isolichenan and also galactomannans [5,8,9]. Many hypotheses have been formulated to explain the role of these carbohydrates in lichens. They might play important functions in thallus water desiccation tolerance [10,11] but more recently they are suspected to be involved in the initiation of symbiosis between both partners [12].

A better understanding of the polysaccharides' functions requires their structural elucidation and actually, methods are currently missing to analyze them directly because of their high molecular weight (HMW) and dispersity. The complexity of producing oligosaccharides from crude polysaccharidic extracts in order to describe their inner structure results from (i) the large variety and number of monomers, being (ii) linked together with various glycosidic linkages which constitutes the principal backbone, and (iii) the addition of branched-chains also having the same complexity (monosaccharide composition and specific glycosidic bonds). In this respect, current mass spectrometry (MS) techniques do not afford the direct characterization of the structure of intact HMW polysaccharides. In addition, intact polysaccharides are so complex that even measuring their mass is challenging with MS, and their MW is generally measured using light scattering techniques such as MALS (multi-angle light scattering) [13]. The fine structural characterization of polysaccharides is therefore generally done using "bottom-up" approaches. First, it is compulsory to separate the different polysaccharides obtained from aqueous extraction according to their size, charge and composition. Then purified polysaccharides should be degraded into oligosaccharides for which much more analytical methods are available [14] mainly LC-MS, NMR analyses or GC and GC-MS after derivatization.

Among the MS-based methods used for analyzing oligosaccharides, matrix-assisted laser desorption/ionization–time-of-flight (MALDI-TOF) MS is of particular interest for fingerprinting after incubation with enzymes [15] Ropartz et al. developed a special ionic matrix to enhance the ionization and repeatability of MALDI analyses of chemically heterogeneous oligosaccharides [16]. Since then, this method has been applied to study the hydrolysis of different polysaccharides (e.g., Refs. [17–21]).

The hydrolysis of polysaccharides into oligosaccharides relies on several crucial steps to obtain an informative profile representative of the monosaccharidic linkages and structural isomerism. Yet, few studies compare the oligosaccharide profiles obtained with different depolymerization approaches. The use of enzymatic processes is popular [22]: for example, it is easy to use α-amylase to obtain malto-oligosaccharides from starch. Nevertheless, it is sometimes more difficult to get hold of a specific enzyme to degrade an unknown polysaccharide given the limited reservoir of glycosidase enzymes available. In the case of lichens, major polysaccharides are either linear and branched and they are formed with α-and β-glucans, α-mannans with (1 → 3), (1 → 4) and (1 → 6) linkages differing in their ratios [12]. Some heteroglycans have also been reported [12]. Such heterogeneity hampered the use of glycosidases for degradation purpose. In our case, some preliminary assays using the commercial enzyme exo-α-(1,2,3,4,6)-D-mannosidase (Megazyme) and the endo-α-(1 → 6)-mannanase (Nzytech) failed to degrade lichen polysaccharides. Another current method is the use of acids (hydrochloric or trifluoroacetic acids) that can easily break the glycosidic linkages. Recently a new method called Fitdog (Fenton's initiation toward defined oligosaccharide groups) based on oxidative cleavage of inter-glycosidic linkage was described as a successful process to obtain oligosaccharides [14] from the trisaccharide up to the octasaccharide. This is an attractive method but considering the reactive species generated during the reaction, the possibility of by-products from intra-glycosidic oxidative cleavage is important. The nature of such by-products was never elucidated so far.

In this context, the oxidative degradation of polysaccharides according to Fitdog's protocol was compared with a more classic acidic one. The polysaccharides extracted from the lichen *L. pustulata* were chosen as a model of study. The depolymerization of the fraction with the highest molecular weight was investigated using MALDI-TOF-MS in addition to HPLC-ELSD for preliminary evaluation in order to analyze the distribution of the released oligosaccharides as well as the nature of the by-products. The same protocol was then applied to *Cetraria islandica* extracted polysaccharides to validate the conclusions about the degradation profiles generated by each hydrolysis technique.

2. Experimental methods

2.1. Materials and chemicals

All lichen samples were collected in France. *Cetraria islandica* (Ci) and *Lasallia pustulata* (Lp) were collected respectively in the Alpes (Haute-Savoie (74), August 2009) and in Aubrac (Saint Urcize, Cantal (15), February 2019). Vouchers were stored in the Herbarium of the laboratory under the codes (JB/09/106) and (JB/19/227).

The solvents acetonitrile (ACN, HPLC grade), *n*-butanol (*n*-BuOH), ethanol (EtOH), formic acid (FA), sulfuric acid, trifluoroacetic acid (TFA), sodium hydroxide (NaOH), glacial acetic acid, sodium acetate, hydrogen peroxide, 2,5-dihydroxybenzoic acid (DHB), $Fe_2(SO_4)_3$ and sodium borohydride were purchased from Sigma-Aldrich (St. Louis, MO). *N,N*-dimethylaniline (DMA) was purchased from Fischer Scientific (Illkirch, France). Ultrapure water (18.3 MΩ-cm at 25 °C) was used for all experiments. All standards oligosaccharides (glucose, mannose, fucose, lactose, maltose, saccharose, laminaritriose, melezitose, stachyose, maltohexaose) were purchased from commercial sources and were used without further purification unless noted.

2.2. Lichen extraction

According to Peyrera et al. [6], thalli of lichens were separated from the support (soil, rocks), washed with water (3x) and dried overnight at 60 °C. 14.8 g of thalli were boiled 30 min at 100 °C (3x) in water and filtrated through cheesecloth. After cooling, the soluble fraction was centrifuged (2.000 g, 15 min). The supernatant was precipitated with EtOH (v/v) and filtrated through a Büchner to afford fraction A. Fraction B1 (>10 kDa) were obtained after ultrafiltration using Amicon device with a regenerated Cellulose Filter (10 kDa, Merck Milipore), a concentration step under vacuum and lyophilization step. They were stored in the dark at room temperature (Fig. S1).

2.3. Size exclusion chromatography (SEC)

SEC system was used to evaluate the molecular size of both fraction B1 of *L. pustulata* and fraction A of *C. islandica*. It consists in an isocratic pump (Malvern Viscotek) equipped with a degaser (Malvern, VE7510) and RI (VE3580, Viscotek), LALS and RALS detectors (Malvern, 270 Dual detector). The column (300 × 8 mm, porous polyhydroxymethacrylate polymer, Malvern) had an exclusion limit of 1000 kDa. The chromatograms were recorded by using OmniSEC

software for peak integration. The mobile phase was 0.1 M $NaNO_3$ solution [7]. 100 µL of the solution of the fractions (1 mg/mL dissolved in distilled water and then filtered through a membrane (0.2 µm, Millipore)) were injected and eluted at a constant flow rate of 1 mL min^{-1}. Two polysaccharide standards of known molecular weights, PEO (PolyCAL PEO Std-PEO-24K Malvern, M_n 23533 Da, M_w 23850 Da) and Dextran (PolyCAL DEXTRAN Std-T-73K Malvern, M_n 53956 Da, M_w 71747 Da) were chosen to calibrate the column.

2.4. Polysaccharides hydrolysis

2.4.1. TFA

The developed method was adapted from Amiccucci et al., 2019 [23]. 20 mg of fraction B1 or A were dissolved in 10 mL ultrapure water and mixed with 10 mL of TFA 100 mM. The hydrolysis was carried out at 100 °C under reflux for: 0, 2, 8 and 24 h, and neutralized with 10 mL of cold 100 mM NaOH.

2.4.2. Fitdog hydrolysis

The method was adapted from several articles by the group of Carlito Lebrilla [14,24]. 10 mg of polysaccharide (fraction B1 or A) were dissolved in 10 mL of a solution obtained by mixing 95 mL of sodium acetate (40 mM), 5 mL of hydrogen peroxide 30 % (v/v) and 3.2 mg of hydrated $Fe_2(SO_4)_3$. The mixture was incubated at 100 °C under agitation and several samplings at various time were realized (0, 10, 20, 30, 40 min). The reaction was stopped by addition of 5 mL of cold NaOH 2M immediately followed by addition of 120 µL of glacial acetic acid. The reaction was realized in an ice bath. Then, oligosaccharides produced during the depolymerization step were reduced at 65 °C using 5 mg $NaBH_4$ for 1 h.

After TFA and Fitdog hydrolyses and before analyses by TLC, MS and injection in HPLC-ELSD, samples were eluted on porous graphitic carbon (PGC) SPE cartridges (SPE Hypercarb, Thermo Scientific 60106-402). The cartridges were conditioned with 4 mL of solution 1 (80 % acetonitrile/TFA 0.2 % in water), then rinsed with 4 mL of HPLC grade water, then the hydrolyzed fraction was first trapped with 10 mL water then eluted with 4 mL of solution 2 (40 % acetonitrile/0.1 % TFA in water) to give the oligosaccharides fraction. The last fraction (eluted with 4 mL ACN …) of each hydrolysis was lyophilized and stored at −20 °C before analysis.

2.5. Analytical methods

2.5.1. Sample preparation

Samples were reconstituted in 100 µL of ultrapure water before high-performance liquid chromatography with evaporative light scattering detector (HPLC-ELSD) analysis.

2.5.2. High performance liquid chromatography coupled to evaporative light scattering detector (HPLC-ELSD)

Polysaccharide depolymerization was studied with an analytical porous graphitic carbon (PGC) column (Hypercarb, 5 µm particles size, 4.6 × 150 mm, Thermo Scientific ref. 35005–154646). Chromatographic separation was performed on a Shimadzu LC-20AD HPLC coupled to an SEDEX LT-ELSD 90LT, with a binary gradient formed with solvent A (H_2O with 0.1 % FA) and solvent B (ACN with 0.1 FA) at a column temperature of 30 °C, and flow rate of 0.5 mL min^{-1}: 3 % B, 0–5 min; 3–6 % B, 5–15 min; 6–10 % B, 15–55 min; 10–50 %B, 55–70 min; 50–90 %B, 70–80 min; 90 %B, 80–85 min; 90-3 % B, 85–90 min; 3 %, 90–95 min. Experimental parameters for the ELSD detection were: photomultiplier gain 3.0, data rate 2 Hz and smoothing 1.0 sec. 20µL of samples were injected at 10 mg/mL. Ten standards representative of oligosaccharides of DPs 1, 2, 3, 4 and 6 were injected (5 µL at 10 mg/mL) to illustrate their dispersion on the column and to be used as quality controls (Fig. S2).

2.5.3. Matrix-assisted laser desorption ionization -mass spectroscopy (MALDI-MS)

Samples were diluted in high-purity deionized water to a concentration of 100 µg/mL (increased to 1 mg/mL for the Fitdog hydrolysis of Cetraria A), then 1 µL was deposited for spot analysis on an MTP 384 target plate (Bruker Daltonics, Bremen, Germany). To each spot was added 1 µL of an *N,N*-dimethylaniline/2,5-dihydroxybenzoic acid (DMA/DHB) ionic matrix (100 mg/mL DHB dissolved in H_2O:ACN:DMA 1:1:0.02 (v/v/v)) [16]. MALDI-MS analyses were performed using a RapiFlex TissueTyper ToF-ToF spectrometer (Bruker Daltonics, Bremen, Germany), which uses a 355 nm laser operating at 10 kHz for ionization. The instrument was calibrated in the *m/z* 300–3200 range using a 100 µg/mL isomaltooligosaccharide mixture (IMOS). Analyses were performed at 38–44 % laser power (increased to 55 % for the TFA hydrolysis of Lasallia B1), sampling 10000 shots randomly across each spot. The spectra were analyzed using FlexAnalysis 4.0 (Bruker Daltonics, Bremen, Germany), the *m/z* ranges of the spectra presented in the different figures were chosen to best represent the oligosaccharide profiles of each sample. The peaks corresponding to the species of interest were picked manually, under the condition that at least two isotopes were resolved.

3. Results

3.1. Extraction of crude polysaccharides extracts and characterization by NMR and HPSEC

Lichen thalli were extracted according to a protocol reported by Peyrera et al. [6] to give crude extracts which precipitated after cooling to give a soluble fraction called A (Fig. S1). Starting with 15 g of lichen led to a quantity of 1.9 g for *L. pustulata* and 5.3 g for *C. islandica* which was 2 to 5-fold higher than for the insoluble fraction, respectively. These results were in agreement with those described by Prieto [25] and Peyrera [6]. Then, precipitation of the soluble fraction with ethanol followed by filtration and ultrafiltration of the filtrate with a cut-off of 10 kDa gave fractions called B1. For the lichen *L. pustulata*, polysaccharides with a molecular weight over 10 KDa served as a model for various depolymerization techniques while maintaining the solubility of the latter. This last ultrafiltration step was not realized for the fraction A of *C. islandica* given its molecular weight (see below).

3.2. HPSEC

Both fractions A and B1 were analyzed for hydrodynamic volume distributions (Fig. S2). Profiles of both chromatograms comprise one peak and the retention volumes were 9.2 mL and 8.3 mL for *L. pustulata* and *C. islandica,* respectively. The chromatograms were used to calculate the weight-averaged (Mw), the number-averaged (Mn) and polydispersity (Mw/Mn). The fraction B1 of *L. pustulata* exhibited a molecular weight (Mw) of 678,596 Da with a polydispersity index (Mw/Mn) of 4 while fraction A from *C. islandica* had a Mw = 130,955 Da with a Mw/Mn = 1.9. All peaks were in the range of the column. The molecular weight was higher than those reported for *C. islandica* by Gorin who reported a degree of polymerization between 100 and 200 (27,000 Da in average) [5]. Environmental variation like harvest time, season were already described as factors to explain the variation of carbohydrate contents in plants [26] but also in algae [27].

3.3. TFA hydrolysis

Liquid chromatography coupled with ELSD (HPLC-ELSD), was used to evaluate the depolymerization of both lichen fractions after TFA hydrolysis. Indeed, it was useful to observe a global distribution of the polysaccharides depending on reaction time and to approximate the polymerization degree of the resulting oligosaccharides thanks to the use of standards (Fig. S3).

The fraction B1 of *L. pustulata* was submitted to TFA hydrolysis during 24 h according to the protocol of Amiccucci et al. Three samplings at 2, 8 and 24 hours were performed in order to follow the kinetics of the depolymerization. The samples were analyzed by HPLC-ELSD (Fig. 1A) along with the mix of controls (Fig. S3). One of the main reasons for using HPLC-ELSD to follow the depolymerization is that it allows detecting carbohydrates species of any size, even very large species that would have been difficult to visualize in MS. In addition, Porous Graphitized Column (PGC) used in the liquid chromatographic separation was adapted to the separation of neutral oligosaccharides [28]. Two phenomenon drove the separation: at low organic solvent concentrations, a dipole–dipole phenomenon prevailed, while at high organic solvent concentrations, it co-existed with a size-exclusion one [29]. At initial time, aside from the injection peak at 3.6 min, two peaks were observed at 6.2 and 63.9 min. In this degradation kinetics, the 60–80 min region of the chromatograms is especially interesting because it exhibits a behavior that is fairly typical of a size-exclusion phenomenon. The second peak at 63.9 min of the t_0 kinetics point presumably corresponds to residual polysaccharide that remained after the SPE filtration. At t = 2 h, two observations can be made: (i) the peak at 63.9 min has shifted to a shorter retention time of 63.2 min, indicating an unfolding under the action of TFA; (ii) a wide degradation envelope has appeared, centered at 66.1 min. At t = 8 h, the peak at 63.2 min has disappeared while the degradation envelope has widened and shifted to a later retention time of 66.4 min, indicating further degradation of the polysaccharide. After 24 h, the degradation envelope finally appeared as a series of sharper peaks spanning between 65 and >70 min (centered at 67.1 min), showing that the TFA hydrolysis continued.

MALDI-TOF-MS analyses confirmed that the TFA degradation of fraction B1 from *L. pustulata* produced oligohexoses, characterized by a Δm 162.06 between related species (corresponding to the mass of a dehydrated hexose subunit). Fig. 1B presents the MALDI mass spectra for the different kinetics times, with a focus on the *m/z* 800–3200 range, where oligosaccharides can be clearly distinguished from the background matrix peaks. No oligosaccharides were detected at initial time, and no significant contribution was observed at t = 2 h either. This is in line with the LC(PGC)-ELSD results that suggest that the species generated after 2 h of hydrolysis are still quite large, and thus fall outside of the analysis range in MALDI. At t = 8 h, a release of oligosaccharides from the polysaccharide is observed, with DPs 3–19 being detected as $[M+Na]^+$ with an envelope centered on DP6 at *m/z* 1013.32 (theoretical *m/z* values for $[M+Na]^+$ of oligohexoses are given in Table S1). In addition to these neutral oligohexoses highlighted in blue in Fig. 1B, MALDI-MS also unveiled the presence of singly, doubly or even triply pentosylated species, highlighted in green and characterized by a Δm 132.04 (e.g., a 6.Hex detected at *m/z* 1013.32 and 6.Hex + 1.Pent detected at *m/z* 1145.35, full-scale spectrum for t = 8 h available in Fig. S4). Finally, MALDI-MS also showed the presence of acetylated oligohexoses (probably linked to the degradation of pustulan), indicated by a red asterisk. Overall, the t = 8 h kinetics point showed a high structural diversity in fraction B1 from *L. pustulata*. At t = 24 h, the MALDI spectrum showed an increase in intensity of the oligohexoses, but the disappearance of the pentosylated and acetylated species, indicating that increased exposure to the TFA results in a loss of structurally relevant moieties.

The same protocol was applied on the fraction A of *C. islandica*. Kinetic was monitored at 2, 8 and 24 h during TFA hydrolysis. As for Lp, the HPLC-ELSD chromatograms confirmed the occurrence of degradation (Fig. 2A). Indeed, at t_0, the chromatogram was almost blank aside from a few peaks of very low intensity between 65 and 70 min. At t = 2 h, a wide peak with shoulder appeared in the same region of the chromatogram, indicating the presence of large species resulting from TFA hydrolysis of the polysaccharide. At t = 8 h, the intensity of the signal in the same 65–70 min region of the chromatogram increased with the apparition of multiple peaks. After 24 h, this profile was still observed but decreased in intensity. Additionally, several early-eluting peaks (Rt = 18, 19, 20, 22, 30, 37, 52 min) were detected, suggesting that TFA hydrolysis yielded relatively small oligosaccharides.

MALDI analyses confirmed the generation of oligohexoses during the TFA hydrolysis of fraction A from *C. islandica*. As depicted in Fig. 2B, MALDI mass spectra show that trace levels of oligohexoses were already present at t_0 of the depolymerization, with DPs of 5–14. No dialysis was performed on the fraction A of Ci explaining the presence of oligohexoses in the crude extract. The mass spectra for the other kinetics points showed that only neutral oligosaccharides were generated during TFA hydrolysis, and clearly illustrated the degradation over time. Indeed, at t = 2 h the degradation envelope was centered on DP10 (*m/z* 1661.53), at t = 8 h it was centered on DP5 (*m/z* 851.26), and at t = 24 h the envelope was finally centered on DP4 (*m/z* 689.21).

3.4. Fitdog method

The fraction B1 of *L. pustulata* was submitted to the Fitdog method [14] at times different from TFA hydrolysis as suggested by preliminary assays. Aliquots at t = 10, 20, 30 and 40 min were retrieved to be analyzed by LC- ELSD. An intense envelope of peaks was seen on the

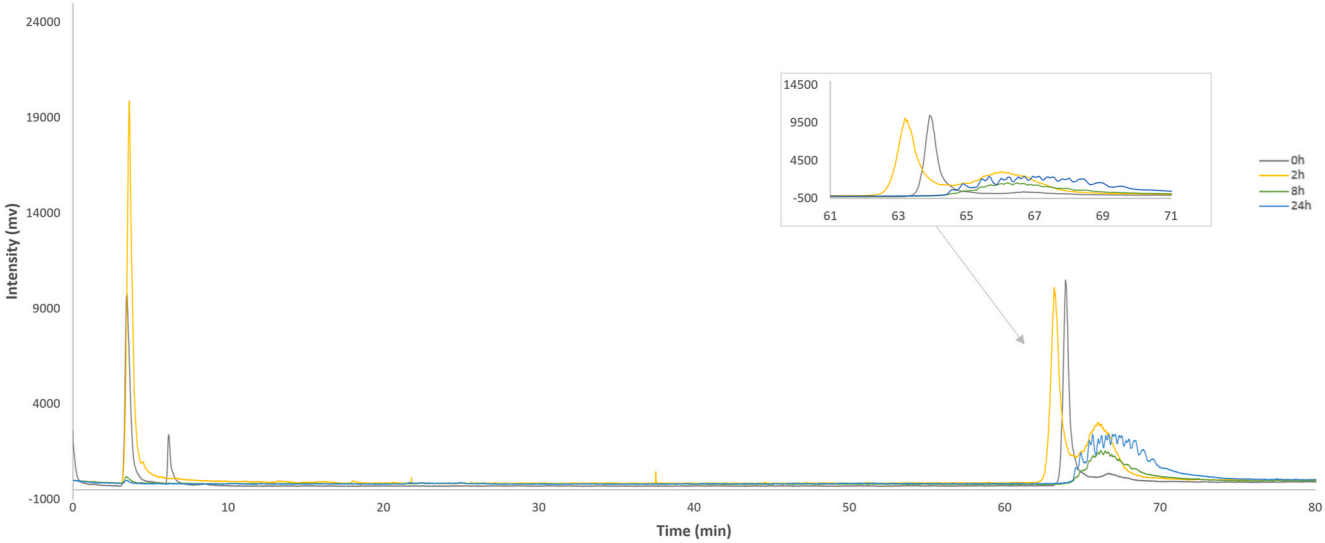

Fig. 1A. HPLC-ELSD of the fraction B1 from *Lasallia pustulata* submitted to the TFA hydrolysis at T = 0, 2, 8, 24 h.

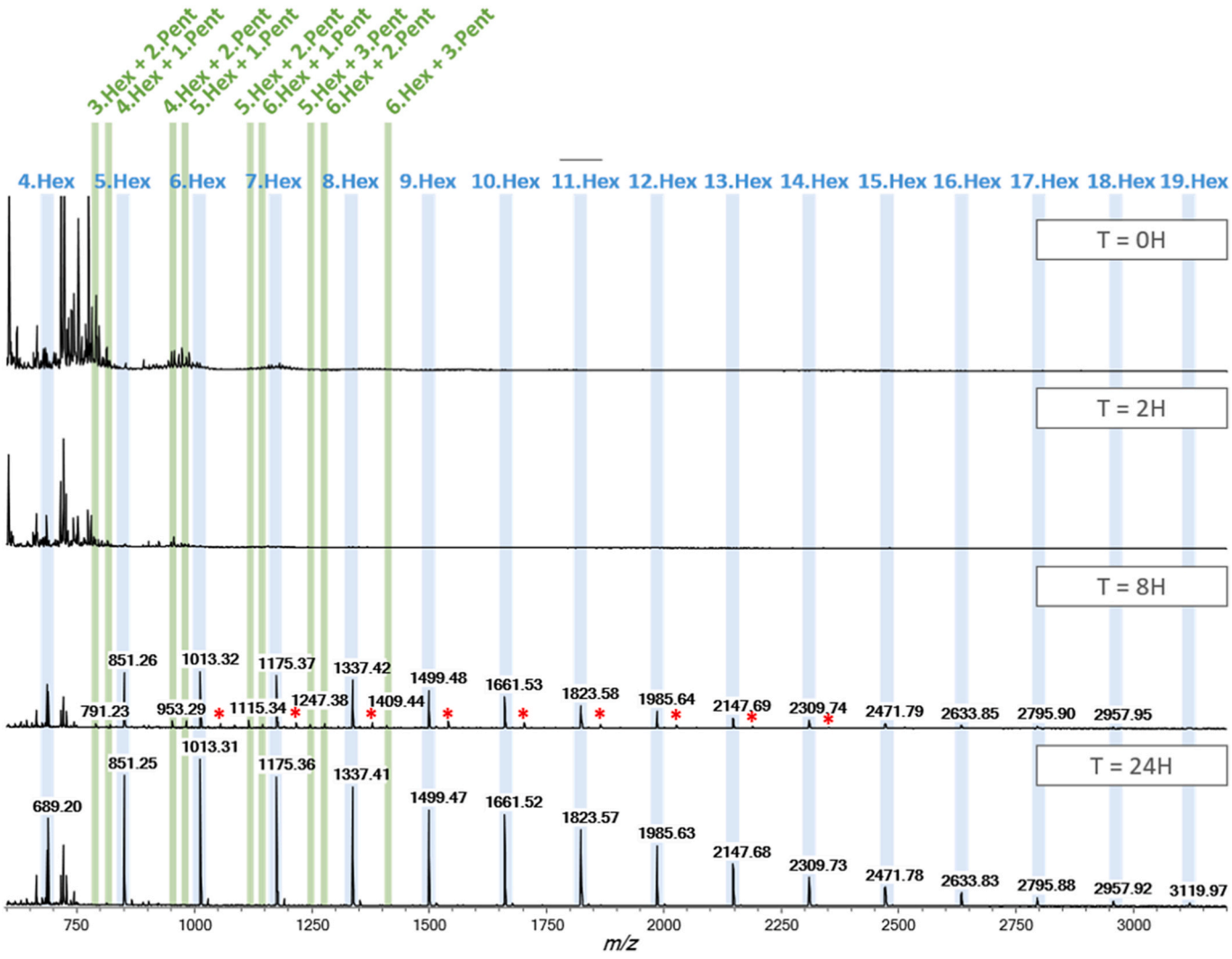

Fig. 1B. MALDI-TOF mass spectra of fraction B1 from *Lasallia pustulata* submitted to TFA hydrolysis at T = 0, 2, 8 and 24 h. All spectra are scaled to an intensity of 20,000 arbitrary units. The masses for different degrees of polymerization of oligohexoses, detected as $[M+Na]^+$, are highlighted in blue and annotated *x*.Hex. Pentosylated species are highlighted in green and annotated *x*.Hex + *x*.Pent (*x* = number of constituting monosaccharides, Hex = hexose, Pent = pentose). Acetylated oligohexoses are indicated by a red asterisk.

chromatograms in the 60–80 min region. In this envelope, where a significant part of the oligosaccharides retained on the column are eluted, the intensity of the peak decreased over time suggesting a depolymerization of the fraction B1 (Fig. 3A). Importantly, the injection peak at *ca.* 4 min was also very intense and was significantly increased at t = 40 min. This suggests that part of the species generated by Fitdog hydrolysis are not retained in PGC (e.g., less polar compounds) and may not be "normal" neutral oligosaccharides. Conversely, some compounds were retained on the column: some peaks at 12, 17, 23, 41, 43, 53, 55, 61, 64 min remained visible at constant retention times after hydrolysis with a slight decrease in intensity. A great number of peaks can also be visualized between 20– 30 min and 50–60 min with retention time (Rt) that differ from each other after 10 min (Fig. 3A), suggesting an evolution over time of the generated structures.

MALDI-MS analyses of the different kinetics points of the Fitdog degradation of the fraction B1 confirmed that different species were generated by Fitdog (Fig. 3B). At t = 10 min, the MALDI mass spectrum showed the presence of multiple components: neutral oligohexoses were observed from DP3 to DP9 with low intensities, alongside with unknown species that also exhibited a Δm of 162.05 As the degradation progressed, the neutral oligohexoses disappeared and the unknown species shifted to lower masses. Finally, after 40 min, no neutral oligohexoses remained and almost all observed species were detected below *m/z* 1000. This indicates that the unknown species are not an artifact, but actually result from the Fitdog process, and will be detailed in the later parts of this article.

The same kinetics times (10, 20, 30, 40 min) were selected for the Fitdog method applied on the fraction A of *C. islandica*. A quick depolymerization was observed on the chromatograms from HPLC-ELSD with the reduction over time of the intensity of the peak Rt = 67 min (Fig. S5). Furthermore, the sum of the areas of the injection peak and the 60–80 min region ssuggested the generation of modified species. The MALDI mass spectra for the Fitdog degradation of the fraction A of *Cetraria* exhibited a very similar profile compared to *Lasallia* B1 (Fig. 4). At t = 10 min, a few neutral oligohexoses were observed (in traces up to DP11), but most of the detected species were unknown. Like for *Lasallia* B1, the mass of these species decreased over time until all species were below *m/z* 1200 at t = 40 min. This very similar behavior between the Fitdog profiles of the two fractions indicates that these unknown species are intrinsically related to this degradation process, and required further investigation.

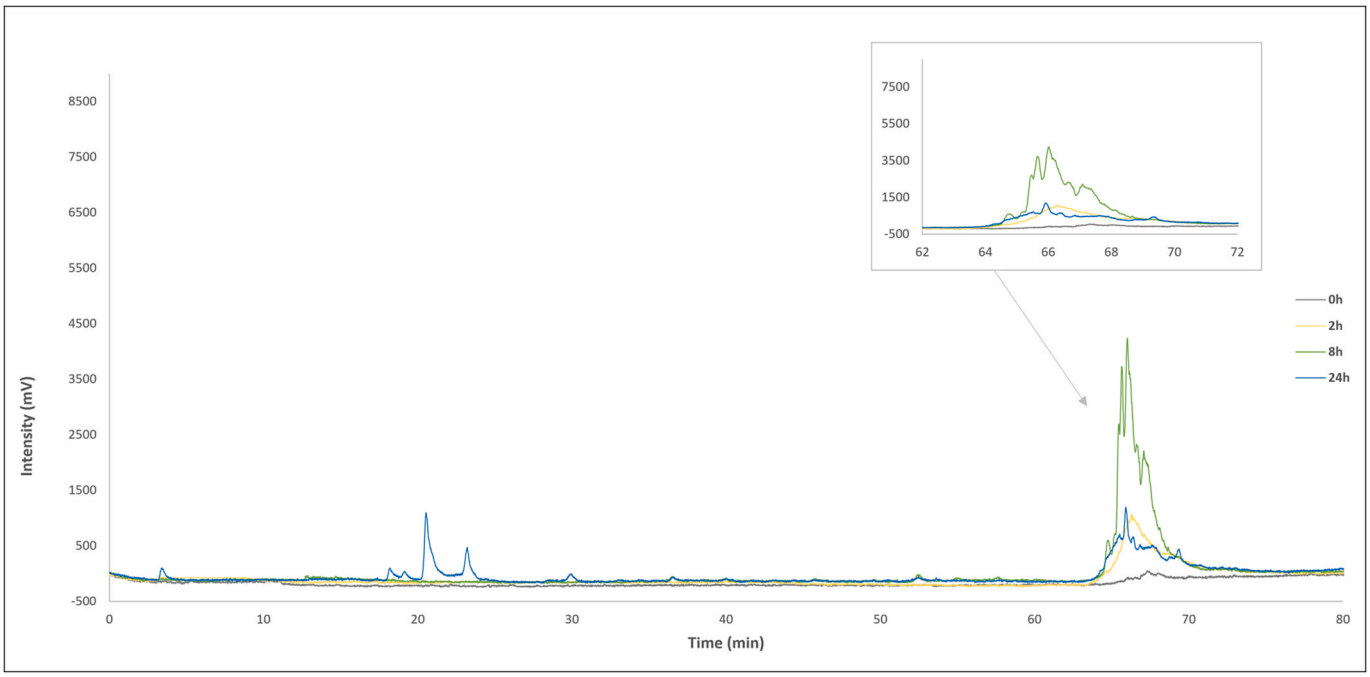

Fig. 2A. HPLC-ELSD of the fraction A from *Cetraria islandica* submitted to the TFA hydrolysis at T = 0, 2, 8, 24 h.

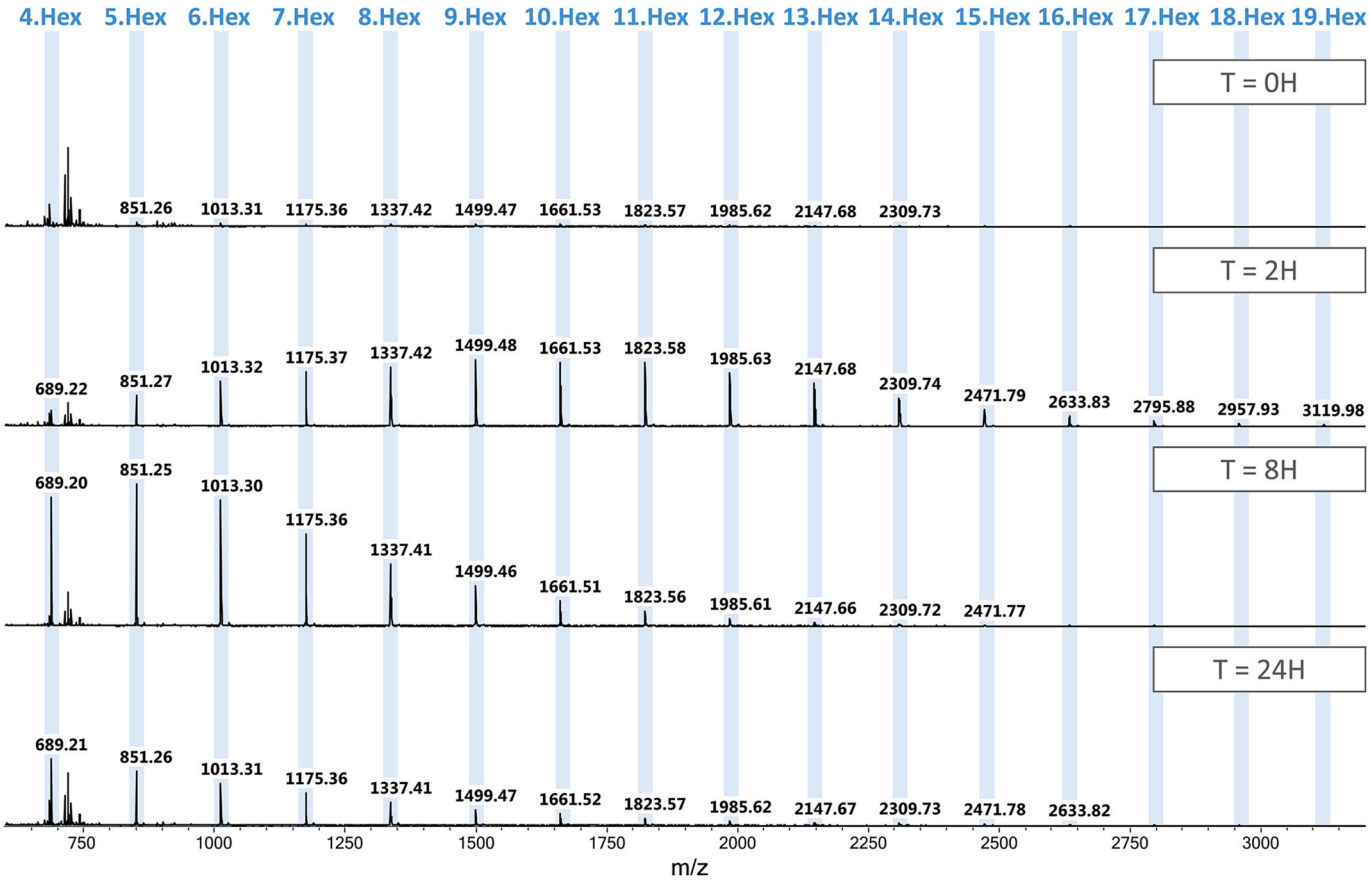

Fig. 2B. MALDI-TOF mass **spectra** of fraction A from *Cetraria islandica* submitted to TFA hydrolysis at T = 0, 2, 8 and 24 h. All spectra are scaled to an intensity of 60,000 arbitrary units. The masses for different degrees of polymerization of oligohexoses, detected as $[M+Na]^+$, are highlighted in blue and annotated *x*.Hex (*x* = number of constituting monosaccharides, Hex = hexose).

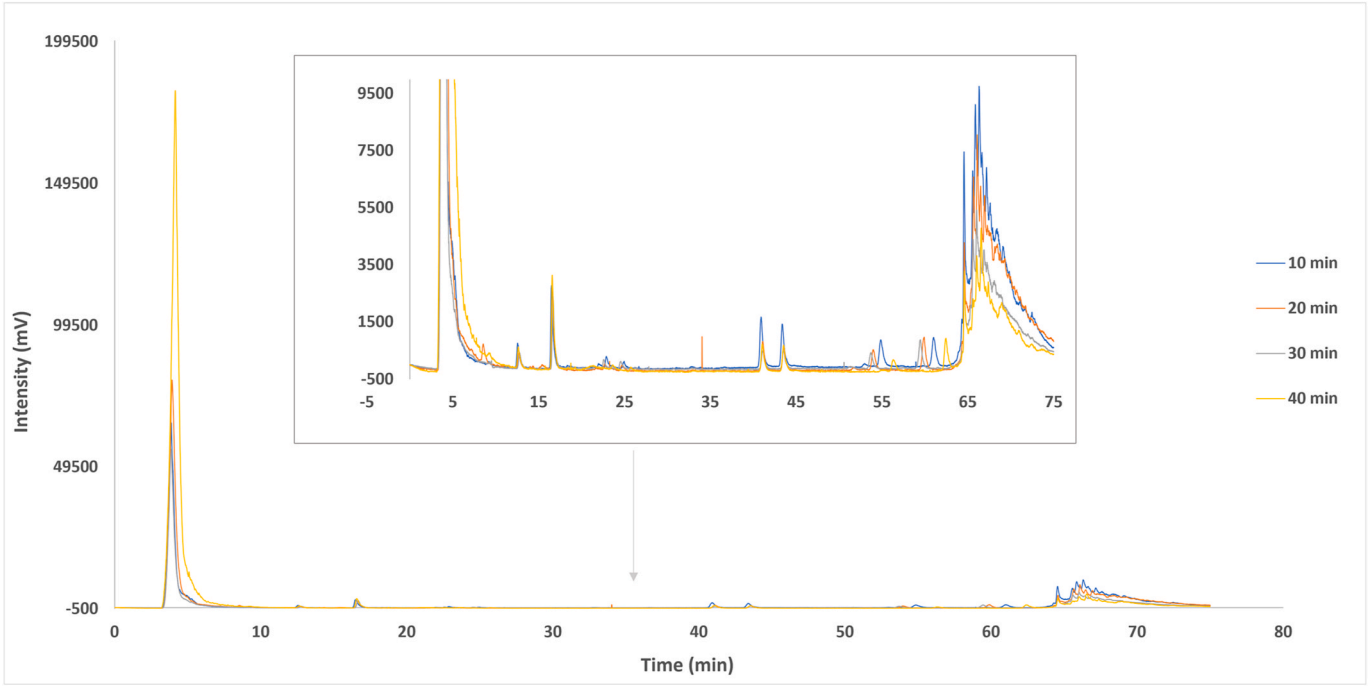

Fig. 3A. HPLC-ELSD of the fraction B1 from *Lasallia pustulata* submitted to the Fitdog hydrolysis at T = 10,20, 30,40 min.

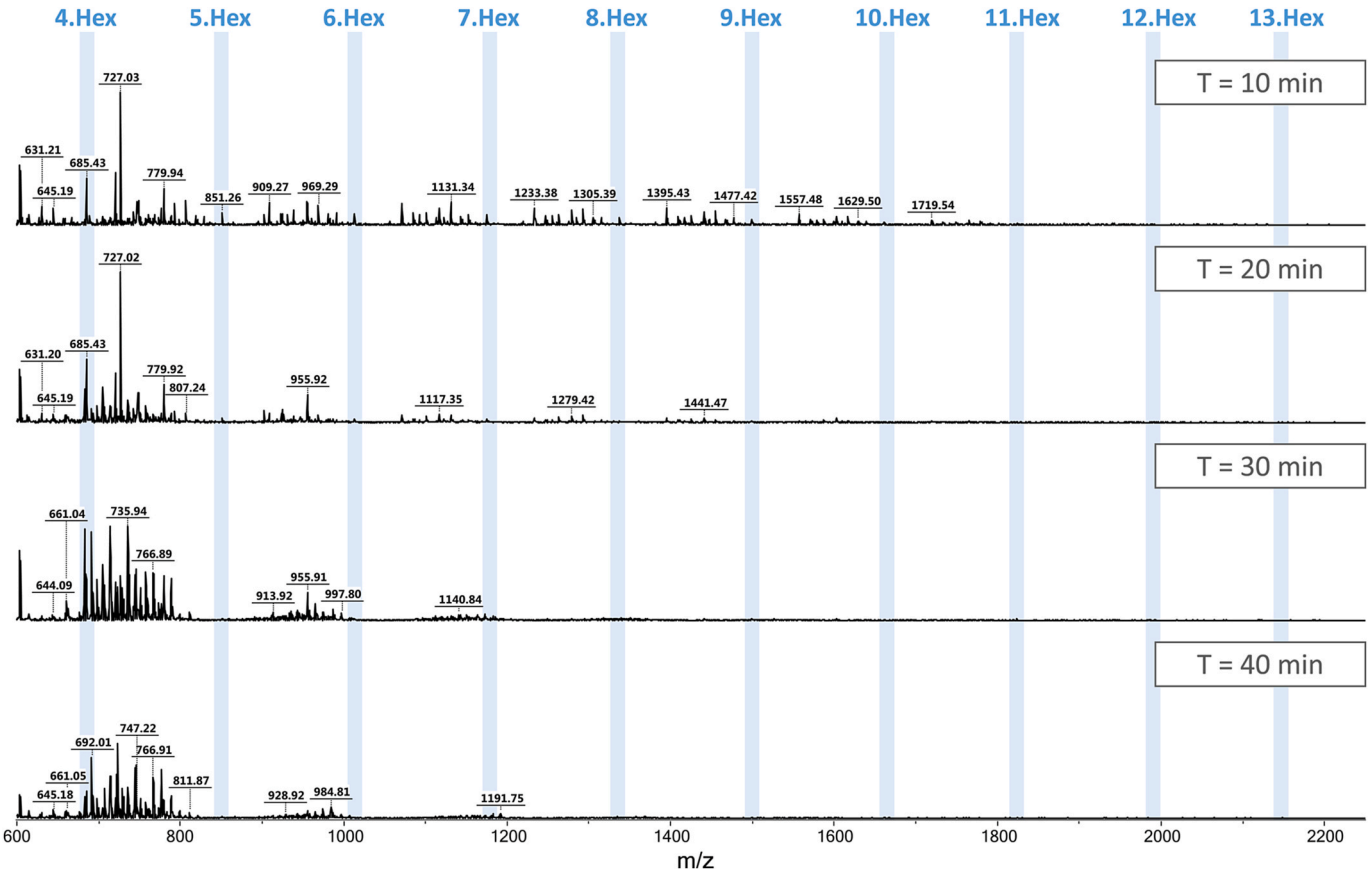

Fig. 3B. MALDI-TOF mass spectra of fraction B1 from *Lasallia pustulata* submitted to Fitdog hydrolysis at T = 10, 20, 30 and 40 min. All spectra are scaled to an intensity of 10,000 arbitrary units. The masses for different degrees of polymerization of oligohexoses, detected as $[M+Na]^+$, are highlighted in blue and annotated *x*. Hex (*x* = number of constituting monosaccharides, Hex = hexose).

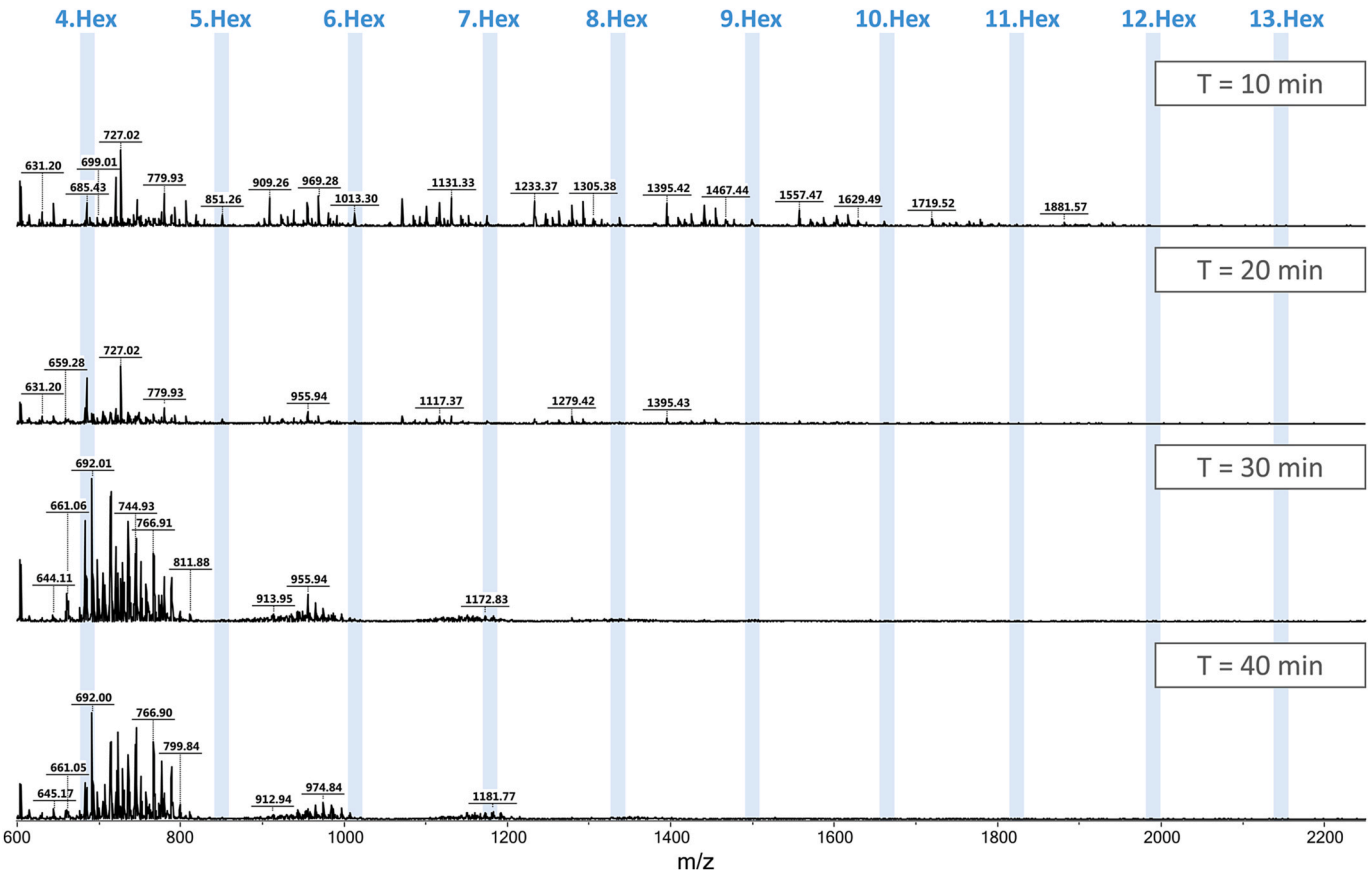

Fig. 4. MALDI-TOF mass spectra of fraction A from *Cetraria islandica* submitted to Fitdog hydrolysis at T = 10, 20, 30 and 40 min. All spectra are scaled to an intensity of 10,000 arbitrary units. The masses for different degrees of polymerization of oligohexoses, detected as $[M+Na]^+$, are highlighted in blue and annotated *x*. Hex (*x* = number of constituting monosaccharides, Hex = hexose).

3.5. Discussion

The degradation of polysaccharides in acidic conditions is one of the earliest methods described so far and is used commonly in the industry [30]. It is known to provide fractions with various polymerization degree and high polydispersity index. Kinetics of the degradation depends strongly of the pH and the temperature. In this context, MALDI analyses, following the TFA hydrolysis of polysaccharides from both *L. pustulata* and *C. islandica*, confirmed the generation of oligosaccharides and the degradation of the polysaccharide as a function of time. Importantly, MALDI also afforded the evaluation of the different types of structures found in each sample: *C. islandica* only contained neutral oligohexoses whereas *L. pustulata* also contained pentosylated and acetylated species.

Depolymerization catalyzed by a metal is wildly used to access sulfated glucosaminoglycan with low molecular weight [31]. In Fenton's reaction, at the heart of the Fitdog method, the reactive species, namely the free hydroxyl radical $OH^{\bullet}$ is generated by action of the metal, here Fe^{3+} on hydrogen peroxide. $OH^{\bullet}$ then abstract a hydrogen from the carbon-hydrogen bond of the polysaccharide. The subsequent action of oxygen induced the oxidative cleavage of the polysaccharide into the oligosaccharides (Fig. S6) [32]. However, such radical-induced oxidative cleavages are likely to occur at the point closest to the position of the radical, which is not necessarily the glycosidic bond as illustrated by Uchida and Kawakishi [33]. Cleavages could therefore occur within the pyranose ring, explaining why the observed masses differ from that expected for neutral oligosaccharides. Such products of over-oxidation were already identified by Lebrilla and co-workers [14] but their exact structures were not deciphered. To further study the modifications induced on the oligosaccharides by the Fitdog reaction, a focus was made on the 10 min kinetics point of the degradation of *L. pustulata* (oligosaccharides are less likely to bear multiple modifications at the earliest point of the degradation). Fig. 5 presents the MALDI mass spectrum for the kinetics point, zoomed-in around DP5. This spectrum exhibits a variety of masses corresponding to modified oligosaccharides, including mass differences that can correspond to a single oxidative cleavage (highlighted in purple) but also masses that can only be produced through more than two consecutive oxidative cleavages (highlighted in red). Compared to unmodified oligohexoses, the masses observed in MALDI-MS notably afforded the identification of losses of CH_4O (*m/z* 819.24), C_2H_4O (*m/z* 807.24), $C_2H_2O_2$ (*m/z* 793.25), $C_3H_6O_3$ (*m/z* 761.23), or $C_4H_8O_3$ (*m/z* 747.22). As hypothesized, these losses can only be generated through intracyclic cleavages occurring on the glycosidic rings either at the reducing end (C_2-C_3 bond *m/z* 819.24 and 793.25), or of the non-reducing end (C_2-C_3 bond *m/z* 747.22, C_3-C_4 bond *m/z* 761.23, C_4-C_5 bond *m/z* 807.24), and some subsequent loss of either glyoxal or dihydroxypropanal. Interestingly no β-alkoxy-elimination could be observed unlike previous finding on cellulose [34]. Possible structural modifications of oligosaccharides derived from pustulan, the main polysaccharide described in both *L. pustulata* and *C. Islandica* were proposed in Fig. 6 (illustrated on a pentasaccharide for conciseness). Of course, these structural propositions remain putative, and each observed mass can come from any proposition, occurring anywhere on the glycosidic chain. Regarding the heterogeneity in the composition and in the nature of the linkage within the considered polysaccharides, the site of chelation of the metal and consequently the selectivity of the cleavage within the hexose is difficult to predict. Nevertheless, the formation of aldehyde following degradation of polysaccharides using Fenton oxidation was already described in the literature confirming the putative structure [35,36]. Recently Lipke et al. confirmed also the formation of aldose/dialdose and

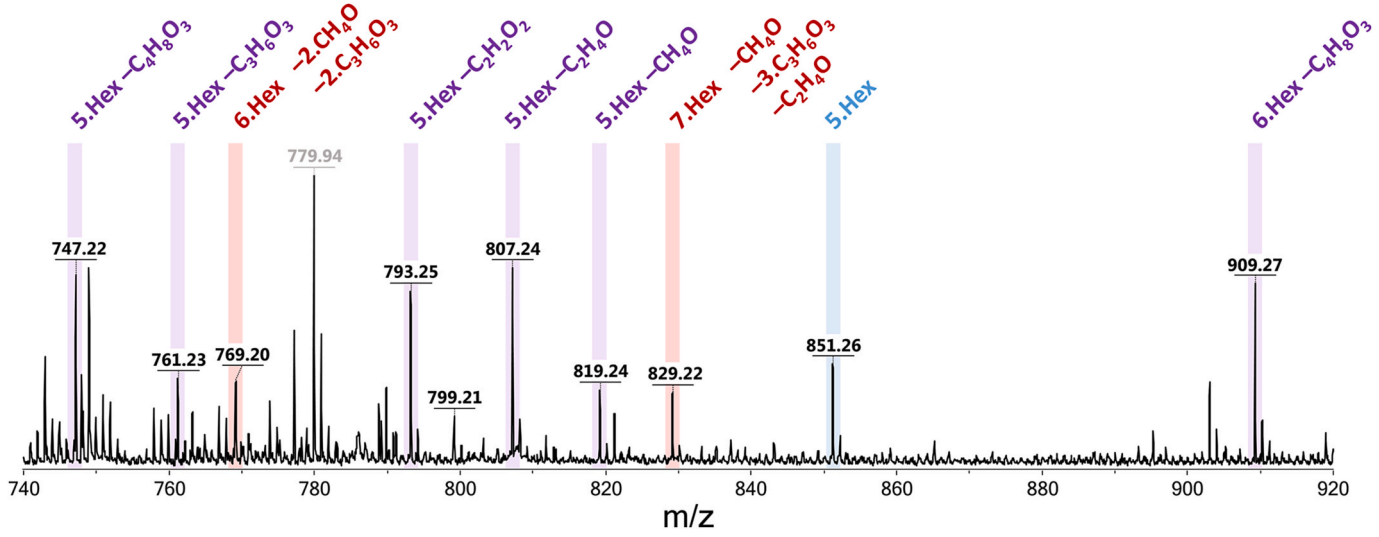

Fig. 5. Zoom-in on the *m/z* range 740–920 of the MALDI-TOF mass spectrum of fraction B1 from *Lasallia pustulata* submitted to Fitdog hydrolysis (T = 10 min). Color code for the masses (as $[M+Na]^+$ species): blue = non-modified oligohexoses; purple = modified oligohexoses bearing a single modification; red = modified oligohexoses bearing multiple modifications.

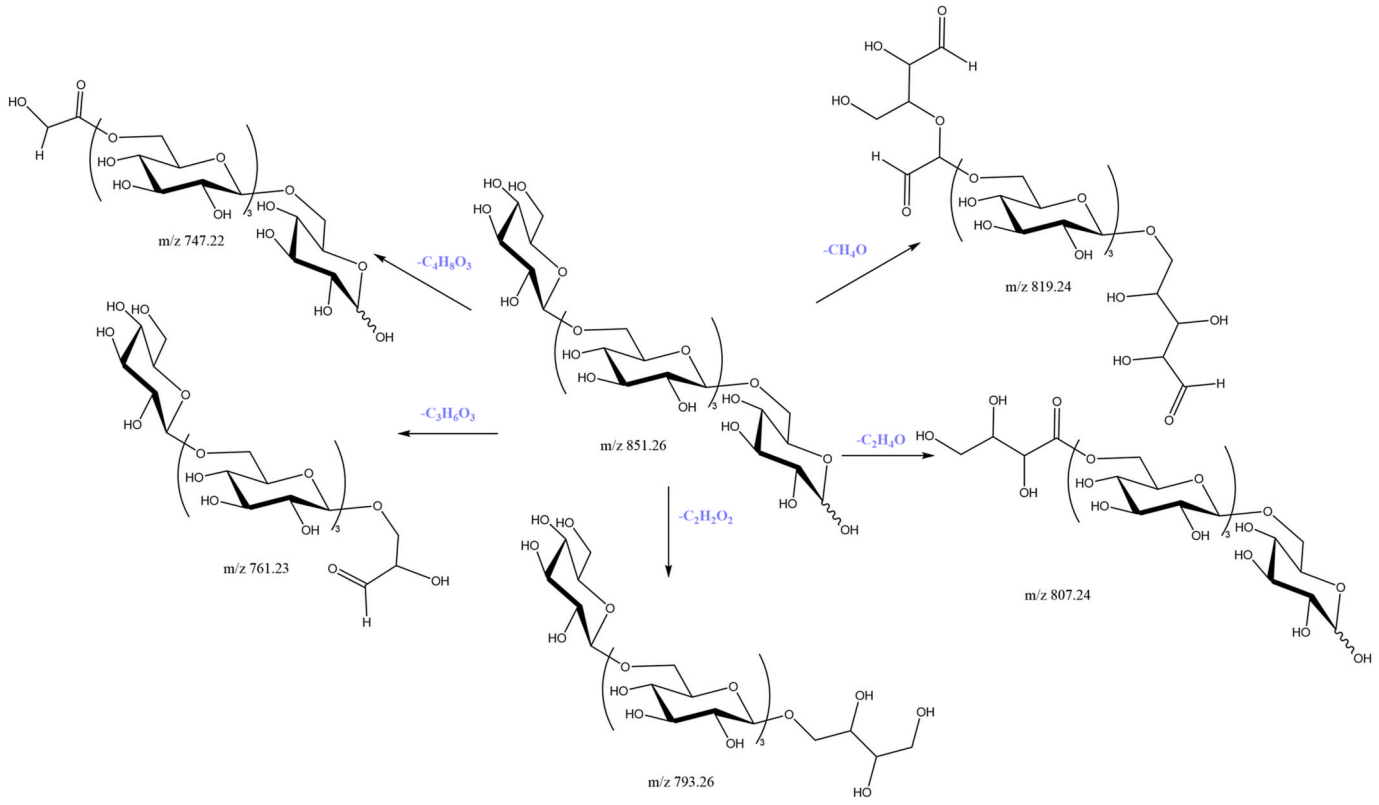

Fig. 6. Putative structures of the various modifications (modified oligohexoses bearing a single modification) identified on the MALDI mass spectrum (to preserve space, the modifications are illustrated on a pustulan pentasaccharide).

uronic/aldonic acids following Fenton oxidation of β-(1 → 3)-glucan [37].

Overall, for the Fitdog hydrolysis of polysaccharides from both *L. pustulata* and *C. islandica*, MALDI analyses afforded the rapid identification of the degradation products, and evidenced that most of the species generated through this reaction were actually modified oligosaccharides bearing either aldehyde or ester function. Such compounds were not identified previously and were not detected using TFA mediated degradation.

4. Conclusion

The reliability of hydrolysis of a mixture of extracted polysaccharides remains a major challenge in order to gain a better understanding of their structural characterization and their involvement in biological phenomena. In this study, MALDI-MS allowed us to quickly discriminate between two methods of hydrolysis in term of implementation and interpretation. It confirms that acid hydrolysis with TFA induced gentle hydrolysis, yielding oligosaccharides with no secondary reaction. It

opens the possibility of future sequencing of the polysaccharide. As for the Fitdog reaction, it is rapid, yielding a wide dispersion of modified neutral oligosaccharides in the two lichens species but inducing concomitant oxidative degradation that should be considered while analyzing the polymer.

CRediT authorship contribution statement

Camille Guitteny: Resources, Methodology, Formal analysis, Writing – original draft, Methodology, Formal analysis, Data curation, Conceptualization. **Simon Ollivier:** Resources, Methodology, Formal analysis, Writing – original draft, Data curation, Writing – review & editing. **Oznur Yeni:** Formal analysis, Data curation. **Mathis Ralaivao:** Formal analysis, Data curation. **Mathieu Fanuel:** Formal analysis, Data curation. **Joël Boustie:** Writing – review & editing, Funding acquisition. **Isabelle Compagnon:** Writing – review & editing, Project administration, Funding acquisition, Conceptualization. **Vincent Ferrières:** Writing – review & editing, Supervision, Project administration, Funding acquisition, Conceptualization. **Solenn Ferron:** Formal analysis, Data curation. **Hélène Rogniaux:** Writing – review & editing, Funding acquisition, Conceptualization. **David Ropartz:** Writing – review & editing, Methodology, Funding acquisition, Conceptualization. **Laurent Legentil:** Writing – original draft, Validation, Supervision, Methodology, Investigation, Funding acquisition, Formal analysis, Conceptualization. **Françoise Le Dévéhat:** Writing – original draft, Supervision, Resources, Methodology, Investigation, Funding acquisition, Formal analysis, Data curation, Conceptualization.

Declaration of competing interest

The authors declare that they have no known competing financial interests or personal relationships that could have appeared to influence the work reported in this paper.

Acknowledgment

The work was supported by Agence Nationale de la Recherche (Project ALGAIMS ANR-18-CE29-0006-02, https://algaims35.webself.net/accueil). Joel Esnault is gratefully acknowledged for lichen pictures.

Appendix A. Supplementary data

Supplementary data to this article can be found online at https://doi.org/10.1016/j.ijms.2025.117473.

Data availability

No data was used for the research described in the article.

References

[1] M.A. de Souza, I.T. Vilas-Boas, J.M. Leite-da-Silva, et al., Polysaccharides in agro-industrial biomass residues, Polysaccharides 3 (2022) 95–120, https://doi.org/10.3390/polysaccharides3010005.
[2] S.-Y. Xu, X. Huang, K.-L. Cheong, Recent advances in marine algae polysaccharides: isolation, structure, and activities, Mar. Drugs 15 (2017) 388, https://doi.org/10.3390/md15120388.
[3] A. Khalid, Asim ur-Rehman, N. Ahmed, et al., Polysaccharide chemistry in drug delivery, endocrinology, and vaccines, Chem. Eur J. 27 (2021) 8437–8451, https://doi.org/10.1002/chem.202100204.
[4] C. Heiss, M.L. Skowyra, H. Liu, et al., Unusual galactofuranose modification of a capsule polysaccharide in the pathogenic yeast *Cryptococcus neoformans*, J. Biol. Chem. 288 (2013) 10994–11003, https://doi.org/10.1074/jbc.M112.441998.
[5] P.A.J. Gorin, E. Barreto-Bergter, The chemistry of polysaccharides of fungi and lichens, in: G.O. Aspinall (Ed.), Hrsg. The Polysaccharides, Academic Press, 1983, pp. 365–409.
[6] M.T. Pereyra, A. Prieto, M. Bernabé, et al., Studies of new polysaccharides from *Lasallia pustulata* (L.) Hoffm, Lichenologist 35 (2003) 177–185, https://doi.org/10.1016/S0024-2829(03)00015-X.
[7] E.R. Carbonero, F.R. Smiderle, A.H.P. Gracher, et al., Structure of two glucans and a galactofuranomannan from the lichen *Umbilicaria mammulata*, Carbohydr. Polym. 63 (2006) 13–18, https://doi.org/10.1016/j.carbpol.2005.04.010.
[8] M. Baron, M. Iacomini, E.S. Fantat, et al., Galactomannan, lichenan and Isolichenan from the polysaccharide -rich lichen *Neuropogon aurantiaco-ater*, Phytochemistry 30 (1991) 3125–3126, https://doi.org/10.1016/S0031-9422(00)98266-9.
[9] L.-P. David, S. Ferron, B. Favreau, et al., Synthesis of galactomannan fragments to help NMR assignment of polysaccharides extracted from lichens, Org. Biomol. Chem. 22 (2024) 2395–2403, https://doi.org/10.1039/d4ob00047a.
[10] R. Honegger, A. Haisch, Immunocytochemical location of the (1→3) (1→4)-β-glucan lichenin in the lichen-forming ascomycete *Cetraria islandica* (Icelandic moss), New Phytol. 150 (2001) 739–746, https://doi.org/10.1046/j.1469-8137.2001.00122.x.
[11] L.M.C. Cordeiro, E. Stocker-WÃ¶rgÃ¶tter, P.A.J. Gorin, et al., Elucidation of polysaccharide origin in *Ramalina peruviana* symbiosis, FEMS Microbiol. Lett. 238 (2004) 79–84, https://doi.org/10.1111/j.1574-6968.2004.tb09740.x.
[12] T. Spribille, G. Tagirdzhanova, S. Goyette, et al., 3D biofilms: in search of the polysaccharides holding together lichen symbioses, FEMS Microbiol. Lett. 367 (2020) fnaa023, https://doi.org/10.1093/femsle/fnaa023.
[13] G.A. Morris, G.G. Adams, S.E. Harding, On hydrodynamic methods for the analysis of the sizes and shapes of polysaccharides in dilute solution: a short review, Food Hydrocoll. 42 (2014) 318–334, https://doi.org/10.1016/j.foodhyd.2014.04.014.
[14] M.J. Amicucci, E. Nandita, A.G. Galermo, et al., A nonenzymatic method for cleaving polysaccharides to yield oligosaccharides for structural analysis, Nat. Commun. 11 (2020) 3963, https://doi.org/10.1038/s41467-020-17778-1.
[15] O. Lerouxel, T.S. Choo, M. Séveno, et al., Rapid structural phenotyping of plant cell wall mutants by enzymatic oligosaccharide fingerprinting, Plant Physiol 130 (2002) 1754–1763, https://doi.org/10.1104/pp.011965.
[16] D. Ropartz, P.-E. Bodet, C. Przybylski, et al., Performance evaluation on a wide set of matrix-assisted laser desorption ionization matrices for the detection of oligosaccharides in a high-throughput mass spectrometric screening of carbohydrate depolymerizing enzymes, Rapid Commun. Mass Spectrom. 25 (2011) 2059–2070, https://doi.org/10.1002/rcm.5060.
[17] M. Fer, A. Préchoux, A. Leroy, et al., Medium-throughput profiling method for screening polysaccharide-degrading enzymes in complex bacterial extracts, J. Microbiol. Methods 89 (2012) 222–229, https://doi.org/10.1016/j.mimet.2012.03.004.
[18] M. Lahaye, X. Falourd, B. Quemener, et al., Cell wall polysaccharide chemistry of peach genotypes with contrasted textures and other fruit traits, J. Agric. Food Chem. 60 (2012) 6594–6605, https://doi.org/10.1021/jf301494j.
[19] M. Lahaye, X. Falourd, B. Quemener, et al., Histological and cell wall polysaccharide chemical variability among apricot varieties, Food Sci Technol 58 (2014) 486–496, https://doi.org/10.1016/j.lwt.2014.04.009.
[20] A. Mishra, M. Joshi, B. Jha, Oligosaccharide mass profiling of nutritionally important *Salicornia brachiata*, an extreme halophyte, Carbohydr. Polym. 92 (2013) 1942–1945, https://doi.org/10.1016/j.carbpol.2012.11.055.
[21] G. Winisdorffer, M. Musse, S. Quellec, et al., Analysis of the dynamic mechanical properties of apple tissue and relationships with the intracellular water status, gas distribution, histological properties and chemical composition, Postharvest Biol. Technol. 104 (2015) 1–16, https://doi.org/10.1016/j.postharvbio.2015.02.010.
[22] R.M. Wahlström, A. Suurnäkki, Enzymatic hydrolysis of lignocellulosic polysaccharides in the presence of ionic liquids, Green Chem. 17 (2015) 694–714, https://doi.org/10.1039/C4GC01649A.
[23] M.J. Amicucci, A.G. Galermo, E. Nandita, et al., A rapid-throughput adaptable method for determining the monosaccharide composition of polysaccharides, Int. J. Mass Spectrom. 438 (2019) 22–28, https://doi.org/10.1016/j.ijms.2018.12.009.
[24] E. Nandita, N.P. Bacalzo, C.L. Ranque, et al., Polysaccharide identification through oligosaccharide fingerprinting, Carbohydr. Polym. 257 (2021) 117570, https://doi.org/10.1016/j.carbpol.2020.117570.
[25] A. Prieto, J.A. Leal, M. Bernabé, et al., A polysaccharide from *Lichina pygmaea* and *L. confinis* supports the recognition of Lichinomycetes, Mycol. Res. 112 (2008) 381–388, https://doi.org/10.1016/j.mycres.2007.10.013.
[26] E.N. Makarova, E.G. Shakhmatov, V.A. Belyy, Seasonal dynamics of polysaccharides in Norway spruce (*Picea abies*), Carbohydr. Polym. 157 (2017) 686–694, https://doi.org/10.1016/j.carbpol.2016.10.035.
[27] L.-E. Rioux, S.L. Turgeon, M. Beaulieu, Effect of season on the composition of bioactive polysaccharides from the brown seaweed *Saccharina longicruris*, Phytochemistry 70 (2009) 1069–1075, https://doi.org/10.1016/j.phytochem.2009.04.020.
[28] C. West, C. Elfakir, M. Lafosse, Porous graphitic carbon: a versatile stationary phase for liquid chromatography, J. Chromatogr. A 1217 (2010) 3201–3216, https://doi.org/10.1016/j.chroma.2009.09.052.
[29] S. Moyses, A. Ginzburg, The chromatography of poly(phenylene ether) on a porous graphitic carbon sorbent, J. Chromatogr. A 1468 (2016) 136–142, https://doi.org/10.1016/j.chroma.2016.09.034.
[30] B. Grandmontagne, Preparation of Citinand/or Chitosan from Shells of Crustaceans or Cephalopods. Patent FR2701029. 1994-08-05, 1994.
[31] N. Volpi, G. Mascellani, P. Bianchini, Low molecular weight heparins (5 kDa) and oligoheparins (2 kDa) produced by gel permeation enrichment or radical process: comparison of structures and physicochemical and biological properties, Anal. Biochem. 200 (1992) 100–107, https://doi.org/10.1016/0003-2697(92)90283-D.
[32] R. Morelli, S. Russo-Volpe, N. Bruno, et al., Fenton-dependent damage to carbohydrates: free radical scavenging activity of some simple sugars, J. Agric. Food Chem. 51 (2003) 7418–7425, https://doi.org/10.1021/jf030172q.

[33] K. Uchida, S. Kawakishi, Interaction of (1+4)- and (l-6) linked disaccharides with the Fenton reagent under physiological conditions, Carbohydr. Res. (1988) 89–99.
[34] T. Hosoya, M. Bacher, A. Potthast, et al., Insights into degradation pathways of oxidized anhydroglucose units in cellulose by β-alkoxy-elimination: a combined theoretical and experimental approach, Cellulose (Lond.) 25 (2018) 3797–3814, https://doi.org/10.1007/s10570-018-1835-y.
[35] Y.H. Song, H.C. Woo, J. Lee, Eco-friendly depolymerization of alginates by H2O2 and high-frequency ultrasonication, Clean Technol 5 (2023) 1402–1414, https://doi.org/10.3390/cleantechnol5040069.
[36] Y.K. Yeung, Y.-R. Kang, B.R. So, et al., Structural, antioxidant, prebiotic and anti-inflammatory properties of pectic oligosaccharides hydrolyzed from okra pectin by Fenton reaction, Food Hydrocoll. 118 (2021) 106779, https://doi.org/10.1016/j.foodhyd.2021.106779.
[37] R. Ovalle, L. Chen, C.E. Soll, et al., Regioselective degradation of [beta] 1,3 glucan by ferrous ion and hydrogen peroxide (Fenton oxidation), Carbohydr. Res. 497 (2020) 108124, https://doi.org/10.1016/j.carres.2020.108124.